Research Article | DOI: 10.5281/zenodo.15652339
www.jnanosam.com

NANOSAM
Journal of NanoScience in Advanced Materials

Optical Properties of $Ga_2Mn_2O_7$ Pyrochlore Ceramic

Kuldeep Singh[1,2#]

We present the first investigation into the optical properties of the $Ga_2Mn_2O_7$ pyrochlore compound, synthesized via solid-state reaction. The optical band gap, derived from reflectance spectra, was determined to be 1.97 eV, indicating its semiconductor behavior. Further optical characterization revealed key parameters including the extinction coefficient (k), skin depth, and refractive index (n) across a broad wavelength spectrum (200 – 800 nm). Additionally, the optical conductivity was systematically evaluated and analyzed. These findings underscore the compound's functional relevance in optoelectronic and protective coating applications.

1. Introduction

Pyrochlore oxides have received significant attention over the last several decades because of their display of a vast array of practically useful properties, including dielectric, photocatalytic, optical, piezoelectric, ferromagnetism, giant magnetoresistance, metal, and ionic conductivity [1–8]. Because of their remarkable physical properties, pyrochlores are used for numerous technological and innovative applications such as luminescence, thermal barrier coatings, sensors, catalysts, and solid oxide fuel cells [9–14]. Their general chemical formula is $A_2B_2O_7$, wherein a trivalent rare-earth/transition metal ion with eight-fold oxygen coordination resides at A-site, and a tetravalent transition metal ion with six-fold oxygen coordination resides at B-site. The sublattice of each of the two metal ions forms infinite, interpenetrating, networks of corner-sharing tetrahedra. Various pyrochlores such as $Bi_2Sn_2O_7$, $Ce_2Sn_2O_7$, $La_2Zr_2O_7$, *etc.*, have been reported to exhibit a high degree of photoactivity [15–17]. Gavrichev et al. found that Sm_2ScTaO_7 is an excellent thermal barrier coating material due to its low thermal conductivity [18]. Coronado *et al.* prepared Bi_2RuMnO_7 and observed that it is a potential cathode material for solid-oxide fuel cells [19]. Among various pyrochlore compounds, manganese-based pyrochlore oxides are prominent functional materials. The scientific as well as industrial communities are interested in these materials due to their low cost, abundance in nature, and vast applications in areas such as optical, electrical, magnetic, magnetic refrigeration, *etc*. [20–23]. For example, $Al_2Mn_2O_7$ was reported to exhibit a ferromagnetic transition and magnetocaloric effect near hydrogen liquefaction temperature [21], whereas the $La_2Mn_2O_{7-\delta}$ compound demonstrated a Griffith-like phase [24]. Khachnaoui *et al.* synthesized $Fe_2Mn_2O_7$ and studied its magnetic and magnetocaloric properties [25]. The pyrochlore compound $Ga_2Mn_2O_7$ stands out as a promising material due to the combined influence of Ga^{3+} and Mn^{4+} ions on its electronic and optical behavior. Tin, as a post-transition metal, contributes to a wide band structure, whereas manganese's partially occupied d-orbitals modulate its light-interaction properties. Their synergistic effects within the pyrochlore lattice give rise to complex electronic transitions, drawing significant interest in optical materials research.

To our knowledge, this is the first study to systematically examine the optical properties of $Ga_2Mn_2O_7$ ceramics. This study focuses on the synthesis and detailed analysis of the optical properties of $Ga_2Mn_2O_7$ pyrochlore ceramic, using techniques such as UV–Vis spectroscopy. The goal is to explore how its unique crystal structure and composition influence light–matter interactions, thereby contributing to the growing body of knowledge in pyrochlore oxide research and paving

[1]*School of Sciences, Noida International University, Greater Noida, Uttar Pradesh-201308, India,* [2]*Department of Physics, Central University of Rajasthan, Bandarsindri, Ajmer-305817, Rajasthan, India*

#Corresponding author: kuldeepsingh.bsc@gmail.com , kuldeep.singh@niu.edu.in

Keywords: Energy bandgap; DRS; Pyrochlore; Optical properties

Received: 02 May 2025 | Accepted: 17 May 2025 | Published online: 26 June 2025

the way for their integration into advanced optical systems.

2. Results and Discussion

Since the structural characterization of GMO pyrochlore ceramic has already been reported previously, the present study focuses on the detailed analysis of their optical behavior [26]. The optical behavior of the synthesized GMO pyrochlore ceramic was investigated using UV–Visible diffuse reflectance spectroscopy (DRS). The reflectance spectrum is shown in Fig.1. It is observed that the reflectance is relatively low in the ultraviolet (UV) region, indicating strong absorption of high-energy photons. As the wavelength increases towards the visible region, the reflectance gradually increases, suggesting reduced photon absorption at lower energies.

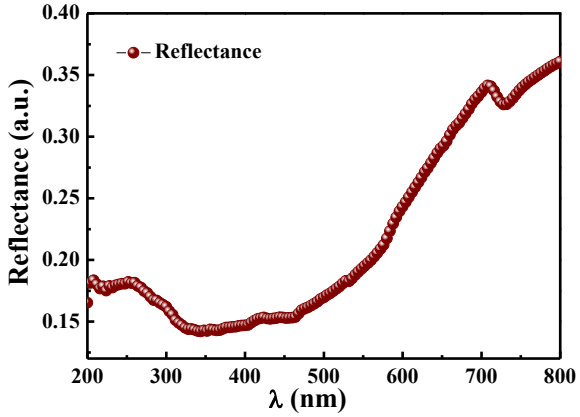

Figure 1. Reflectance spectrum of GMO compound.

The energy band gap was derived using the Kubelka-Munk (K-M) function, where the diffuse reflectance data was transformed into the K-M function via the given equation:

$$\frac{K}{S} = \frac{(1-R)^2}{2R} = F(R) \qquad (1)$$

Here, K (molar absorption coefficient), S (scattering coefficient), and $F(R)$ (Kubelka-Munk function) are the key parameters in the equation. The band gap was determined by plotting $[F(R)h\nu]^2$ against incident photon energy, and the results presented in Fig. 2. The band gap was found to be 3.06 eV. The nature of the optical transition was determined using the following relation:

$$\ln[F(R)h\nu] = p\ ln(h\nu - E_g) \qquad (2)$$

Figure 3 portrays the plot of $\ln(F(R)h\nu)$ *vs.* $ln(h\nu - E_g)$. The fitted straight line's slope (p) yields a value about 0.5. The analysis conclusively demonstrates the direct band gap nature of the studied semiconductor material.

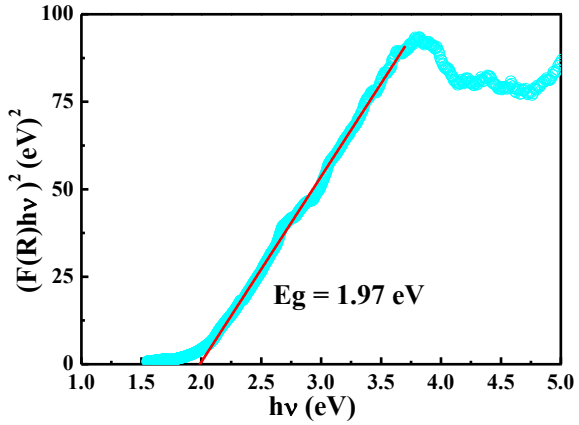

Figure 2. $(F(R)h\nu)^2$ *vs.* incident photon energy for GMO compound.

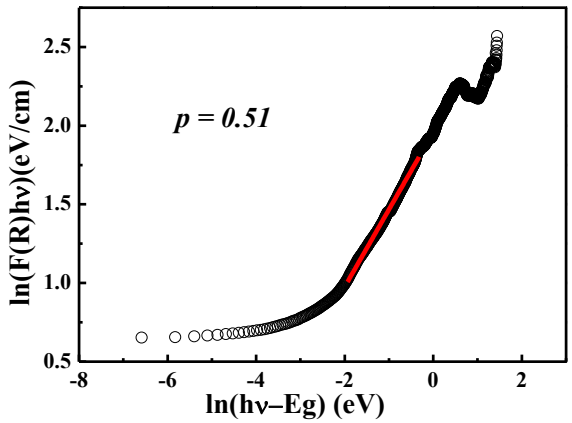

Figure 3. The variation of $(F(R)h\nu)$ versus $\ln(h\nu - E_g)$.

When a conductive material is subjected to high-intensity radiation, the incident electromagnetic waves diminish exponentially as they penetrate the material. This attenuation is measured by the skin depth (δ), which represents the depth at which the wave's intensity drops to 1/e (approximately 37%) of its initial surface value. The skin depth and absorption coefficient (α) are inversely related, expressed by the equation: $\delta = 1/\alpha$. Figure 4 illustrates how the skin depth (δ) of the GMO compound changes with increasing incident photon energy. The graph shows that skin depth decreases as photon energy rises. This occurs because higher-energy electromagnetic waves interact more intensely with the material, enhancing absorption and scattering effects. As a result, the incident energy dissipates more quickly, reducing the wave's penetration depth. Thus, the skin depth becomes smaller at higher photon energies due to the material's stronger attenuation of the electromagnetic waves.

The extinction coefficient (k) measures a material's ability to absorb or reflect electromagnetic radiation at a given wavelength and is determined by the equation: $k = \alpha\lambda/4\pi$. where α is the absorption coefficient and λ is the wavelength. Figure 4 shows the variation of the extinction coefficient with incident photon energy. The graph reveals that k reaches its highest value at lower energies and gradually declines as energy increases. The peak extinction coefficient in this study was found to be 72.1 × 10^{-5}, indicating weak absorption. These low k values confirm the material's high transparency. This trend aligns with observations in other materials, where the extinction coefficient similarly decreases with rising photon energy [27,28]. The extinction coefficient value for GMO was found to be in the range of ~10^{-5}, which is significantly lower than those reported for other oxide materials such as TiO_2 (~10^{-2}) or Fe_2O_3 (~10^{-3} to 10^{-2}) in the visible region. This substantial difference in k values confirms that GMO exhibits superior optical transparency, making it a suitable candidate for applications in transparent coatings, optoelectronic devices, and UV sensors.

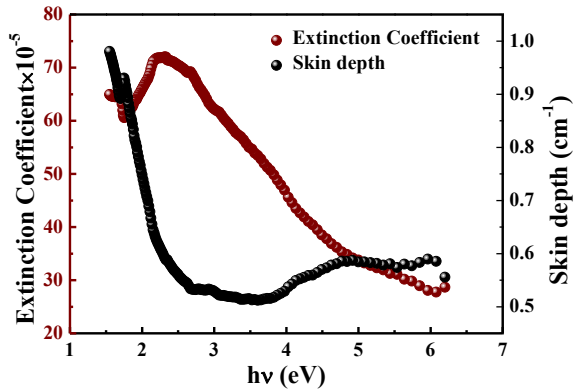

Figure 4. Skin depth and extinction coefficient variation with energy for GMO compound.

The complex refractive index, denoted as $\tilde{n}$ (= $n+ik$), serves as a fundamental optical parameter characterizing a material's interaction with light. The real part (n), representing the standard refractive index, quantifies the reduction in light's phase velocity within the material compared to a vacuum. The imaginary part (k), termed the extinction coefficient, measures energy loss due to absorption or scattering per unit propagation distance. This behavior arises from electronic polarization of ions and the local electric field within the material. The reflection coefficient at normal incidence can be calculated using the relation [29]:

$$R = \frac{(n-1)^2+k^2}{(n+1)^2+k^2} \quad (3)$$

The value of k is very low (~10^{-5}) for the present sample; therefore, Eq. (3) may be written as:

$$n = \frac{(1+R^{\frac{1}{2}})}{(1-R^{\frac{1}{2}})} \quad (4)$$

Figure 5 presents the variation of refractive index (n) with incident wavelength. The refractive index spectrum of GMO reveals a distinct trend where n is relatively low in the UV region but increases gradually with wavelength. This behavior contrasts with typical normal dispersion observed in many dielectric materials. The observed trend may be attributed to the large band gap of the material, which minimizes electronic absorption in the UV range. As the wavelength increases, increased polarizability due to lattice contributions or possible defect-related states may enhance light–matter interaction, leading to a rising refractive index. The observed refractive index behavior positions GMO as an interesting candidate for further optical studies and potential applications where unconventional dispersion characteristics are advantageous.

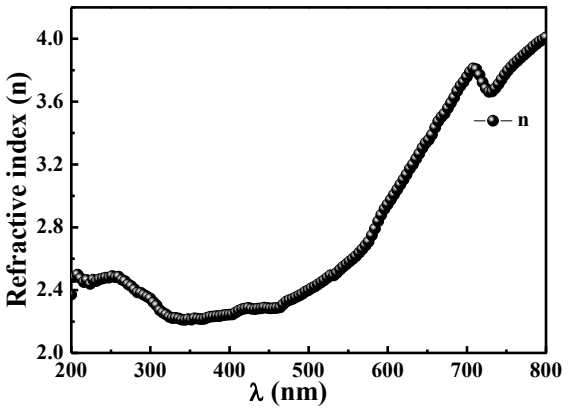

Figure 5. Refractive index variation with wavelength for GMO compound.

Optical conductivity (σ) describes how a material responds to an oscillating electric field (like light) and how it conducts electricity as a function of frequency or photon energy. It strongly depends on several optical parameters such as refractive index, absorption coefficient, and the frequency of incident photons. It has been calculated using the following formula

$$\sigma = \frac{\propto nc}{4\pi} \quad (5)$$

Figure 6 shows the variation of optical conductivity as a function of wavelength for the synthesized GMO pyrochlore ceramic. It is observed that the optical conductivity is relatively high in the

ultraviolet region and decreases progressively with increasing wavelength. This trend indicates strong interaction between high-energy UV photons and the electronic states of the material, facilitating interband transitions. The elevated optical conductivity in this region is attributed to enhanced charge carrier excitation across the band gap or to higher defect states. As the wavelength increases (i.e., photon energy decreases), the likelihood of such transitions reduces, resulting in lower optical conductivity in the visible regions. These observations are consistent with the reflectance behavior, further confirming the material's semiconducting nature and wide band gap characteristics. Owing to these optical characteristics, GMO shows promise for applications in UV photodetectors, solar-blind sensors, and other optoelectronic devices requiring strong UV sensitivity.

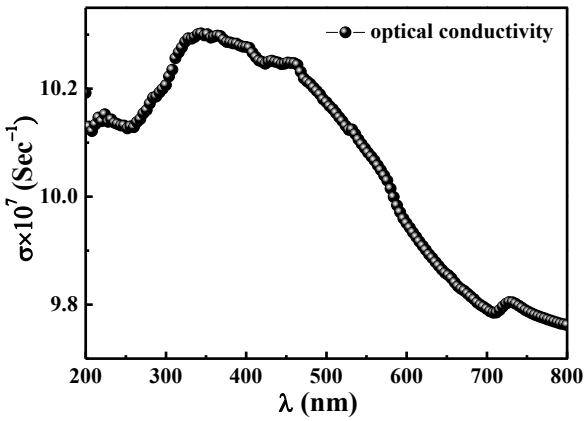

Figure 6. Optical conductivity as a function of wavelength.

3. Conclusion

The polycrystalline $Ga_2Mn_2O_7$ compound was successfully synthesized via the solid-state reaction route. Optical characterization confirmed a direct bandgap transition, as determined from Tauc's plot. In-depth analysis of the extinction coefficient and skin depth as functions of photon energy revealed that the material exhibits low extinction in the visible region, indicating high optical transparency. Furthermore, critical optical parameters, including refractive index and optical conductivity, were systematically investigated as functions of wavelength. These results provide valuable insight into the optical behavior of $Ga_2Mn_2O_7$ and highlight its potential for applications in optoelectronic and UV-responsive devices.

Method

$Ga_2Mn_2O_7$ [GMO] pyrochlore ceramic was prepared by conventional solid-state reaction route from Ga_2O_3 and MnO_2 precursors. Stoichiometric amounts of high purity (99.99%, Sigma Aldrich, USA) powders were mixed and ground by agate mortar pestle. The mixed powder underwent heat treatment ranging from 700, 900, and 1000 °C for 12 hours each time, followed by intermediate grindings after each temperature step. Ultimately, the calcined powder was re-ground and compacted into uniform cylindrical pellets with a diameter of 10 mm, which were then sintered at 1100 °C for 24 hours. To examine the phase purity and structural properties of the material, X-ray diffraction patterns were obtained using an X-ray diffractometer (PANalytical-Empyrean, Netherlands) equipped with Cu Kα radiation (λ = 1.5404 Å) and a scan step of 0.01° per second. In order to measure the optical properties, UV/visible spectrophotometer (Cary series spectrophotometer, Agilent Technologies) was used to obtain the diffuse reflectance spectra (DRS) of the material at room temperature from 200 – 800 nm wavelength range. Barium Sulphate ($BaSO_4$) was utilized as a reference material.

Acknowledgements

This work utilized the facilities provided under the project No. ECR/2017/002681 from DST SERB New Delhi. The authors acknowledge Central University Haryana (India) for the use of DRS facility.

Author Contributions

KS: Performed experiments/data collection, data analysis and interpretation, drafted the paper.

Data Availability Statement

The data that support the findings of this study are available from the corresponding author upon reasonable request.

Declaration of Ethical Standards

The author(s) of this article declare that the materials and methods used in this study do not require ethical committee permission and/or legal-special permission.

Conflict of Interest

The author declares no conflict of interest.

References

[1] Cagnon, J., Boesch, D., Finstrom, N., Nergiz, S., Keane, S., Stemmer, S., Microstructure and dielectric properties of pyrochlore Bi2Ti2O7 thin films, J. Appl. Phys. **102**, 44102 (2007).

[2] Wang, Q., Cheng, X., Li, J., Jin, H., Hydrothermal synthesis and photocatalytic properties of pyrochlore Sm2Zr2O7 nanoparticles, J. Photochem. Photobiol. A Chem. **321,** 48–54 (2016).

[3] Cao, N., Timusk, T., Raju, N., Greedan, J., Gougeon, P., Optical properties of pyrochlore oxides R2Mo2O7-delta (R: Sm, Gd, and Ho), J. Phys. Condens. Matter. **7**, 2489 (1995).

[4] Matteucci, F., Cruciani, G., Dondi, M., Baldi, G., Barzanti, A., Crystal structural and optical properties of Cr-doped Y2Ti2O7 and Y2Sn2O7 pyrochlores, Acta Mater. **55**, 2229–2238 (2007).

[5] Öztürk, E., Karacaoglu, E., Kalem, V., Photoluminescence and piezoelectric behaviour of Y2Zr2O7 pyrochlore-based multifunctional materials and the influence of Eu3+ and Sm3+, Luminescence. 35, 406–411 (2020).

[6] Bongers, P., Van, E., Ferromagnetism in compounds with pyrochlore structure, J. Appl. Phys. **38**, 944–945 (1967).

[7] Shimakawa, Y., Kubo, Y., Manako, T., Giant magnetoresistance in Ti2Mn2O7 with the pyrochlore structure, Nature **379**, 53–55 (1996).

[8] Tuller, H., Mixed ionic-electronic conduction in a number of fluorite and pyrochlore compounds, Solid State Ionics. **52**, 135–146 (1992).

[9] Ćulubrk, S., Antić, Ž., Marinović-Cincović, M., Ahrenkiel, P., Dramićanin, M., Synthesis and luminescent properties of rare earth (Sm3+ and Eu3+) Doped Gd2Ti2O7 pyrochlore nanopowders, Opt. Mater. (Amst). **37**, 598–606 (2014).

[10] Blasse, G., Keulen, J., Luminescence properties of Eu2Sn2O7, Chem. Phys. Lett. **124**, 534–537 (1986).

[11] Yang, J., Han, Y., Shahid, M., Pan, W., Zhao, M., Wu, W., Wan, C., A promising material for thermal barrier coating: Pyrochlore-related compound Sm2FeTaO7, Scr. Mater. **149**, 49–52 (2018).

[12] Jiang, L., Wang, C., Wang, J., Liu, F., Lv, S., You, R., Yao, D., Yan, X., Wang, C., Sun, P., Ultrathin BiVO4 nanosheets sensing electrode for isopropanol sensor based on pyrochlore-Gd2Zr2O7 solid state electrolyte, Sensors Actuators B Chem. **321**, 128478 (2020).

[13] Zhang, J., Wang, D., Lai, L., Fang, X., Xu, J., Xu, X., Zhang, X., Liu, J., Peng, H., Wang, X., Probing the reactivity and structure relationship of Ln2Sn2O7 (Ln= La, Pr, Sm and Y) pyrochlore catalysts for CO oxidation, Catal. Today. **327**, 168–176 (2019).

[14] Anantharaman, A., Dasari, H., Potential of pyrochlore structure materials in solid oxide fuel cell applications, Ceram. Int. **47**, 4367–4388 (2021).

[15] Guo, H., Niu, C., Zhang, L., Wen, X., Liang, C., Zhang, X., Guan, D., Tang, N., Zeng, G., Construction of direct Z-scheme AgI/Bi2Sn2O7 nanojunction system with enhanced photocatalytic activity: accelerated interfacial charge transfer induced efficient Cr (VI) reduction, tetracycline degradation and Escherichia coli inactivation, ACS Sustain. Chem. Eng. **6**, 8003–8018 (2018).

[16] Jayaraman, V., Palanivel, B., Ayappan, C., Chellamuthu, M., Mani, A., CdZnS solid solution supported Ce2Sn2O7 pyrochlore photocatalyst that proves to be an efficient candidate towards the removal of organic pollutants, Sep. Purif. Technol. **224**, 405–420 (2019).

[17] Xu, B., Debao, L., Liyan, G., Feifei, Z., Lijie, Q., Yiguang, W., Baosheng, X., Shigang, A., Synthesis and characterization of novel porous La2Zr2O7 ceramic with ultralow thermal conductivity and excellent photocatalytic property, PREPRINT (Version 1) available at Research Square [https://doi.org/10.21203/rs.3.rs-820717/v1].

[18] Gavrichev, K., Shlyakhtina, A., Khoroshilov, A., Tyurin, A., Ashmarin, A., Konysheva, E., Thermal expansion and heat capacity of Sm2ScTaO7–A promising material for thermal barrier coatings, J. Am. Ceram. Soc. **102**, 4415–4420 (2019).

[19] Martínez-Coronado, R., Alonso, J., Cascos, V., Fernández-Díaz, M., Crystal and magnetic structure of the Bi2RuMnO7 pyrochlore: A potential new cathode for solid oxide fuel cells, J. Power Sources. **247**, 876–882 (2014).

[20] Dwivedi, V., Mukhopadhyay, S., Study of optical properties of polycrystalline Y2Ir2O7, AIP Conf. Proc. , 90016 (2017).

[21] Khachnaoui, F., Amor, N., Nouri, K., Bejar, M., Dhahri, E., Investigation of Griffiths-like phase at low temperature in a new magnetocaloric compound, Al2Mn2O7, J. Phys. Chem. Solids. **148**, 109605 (2021).

[22] Husain, S., Khan, M., Study of Structural and Electrical Transport Properties of Sn Doped La2Mn2O7, J. Optoelectron. Adv. Mater. **10**, 1659–1662 (2008).

[23] Dai, S., Li, Z., Morrish, A., Zhou, X., Zhao, J., Xiong, X., Colossal magnetoresistance in (La0.7Sn0.3)2Mn2O7, Phys. Rev. B. **55**, 14125 (1997).

[24] Khachnaoui, F., Amor, N., Bejar, M., Dhahri, E., Hlil, E., Appearance of Griffiths-Like Phase in a New Pyrochlore Compound La2Mn2O7−δ, J. Supercond. Nov. Magn. **32**, 2133–2139 (2019).

[25] Khachnaoui, F., Amor, N., Bejar, M., Dhahri, E., Hlil, E., Synthesis and Magnetic Properties of New Pyrochlore Fe2Mn2O7 Compound, J. Supercond. Nov. Magn. **31**, 3803–3808 (2018).

[26] Singh, K., Panwar, N., Observation of Griffiths phase, spin glass behaviour and magnetocaloric effect in frustrated Ga2Mn2−xCrxO7 (x= 0, 0.1, 0.3, 0.5) pyrochlore compounds, Curr. Appl. Phys. **53**, 86-93 (2023).

[27] Hcini, F., Hcini, S., Almoneef, M., Dhaou, M., Alshammari, M., Mallah, A., Zemni, S., Lefi, N., Bouazizi, M., Thermal, microstructural, optical, magnetic and magnetocaloric studies for Ni0.5Mn0.5Cr2O4 chromite spinel prepared using sol-gel method, J. Mol. Struct. **1243**, 130769 (2021).

[28] Souifi, K., Rejaiba, O., Amorri, O., Nasri, M., Alzahrani, B., Bouazizi, M., Khirouni, K., Khelifi, J., Detailed Investigation of Structural, Morphology, Magnetic, Electical and Optical Properties of the Half-Doped Perovskite Nd0.5Ba0.5FeO3, J. Inorg. Organomet. Polym. Mater. **32**, 4515–4531 (2022).

[29] Alqahtani, A., Husain, S., Somvanshi, A., Khan, W., Structural, morphological, thermal and optical investigations on Mn doped GdCrO3, J. Alloys Compd. **804**, 401–414 (2019).